The Role of Tropical Waves in Tropical Cyclogenesis

WILLIAM M. FRANK

Department of Meteorology, The Pennsylvania State University, University Park, Pennsylvania

PAUL E. ROUNDY

CIRES, University of Colorado, Boulder, Colorado

(Manuscript received 7 October 2005, in final form 23 December 2005)

ABSTRACT

This paper analyzes relationships between tropical wave activity and tropical cyclogenesis in all of the earth's major tropical cyclone basins. Twenty-nine years of outgoing longwave radiation data and global reanalysis winds are filtered and analyzed to determine statistical relationships between wave activity in each basin and the corresponding cyclogenesis. Composite analyses relative to the storm genesis locations show the structures of the waves and their preferred phase relationships with genesis. Five wave types are examined in this study, including mixed Rossby–gravity waves, tropical-depression-type or easterly waves, equatorial Rossby waves, Kelvin waves, and the Madden–Julian oscillation. The latter is not one of the classical tropical wave types, but is a wavelike phenomenon known to have a strong impact on tropical cyclogenesis. Tropical cyclone formation is strongly related to enhanced activity in all of the wave filter bands except for the Kelvin band. In each basin the structure of each composite wave and the phase relationship between the wave and cyclogenesis are similar, suggesting consistent forcing mechanisms. The waves appear to enhance the local circulations by increasing the forced upward vertical motion, increasing the low-level vorticity at the genesis location, and by modulating the vertical shear. Convective anomalies of waves associated with genesis are detectable in the analyses as long as 1 month prior to genesis. This opens up the possibility of developing statistically based genesis forecasts.

1. Introduction

a. Background

Every year approximately 80 tropical cyclones form over the tropical oceans (Gray 1985). Virtually all of them form over warm, tropical waters in locations that are all but devoid of in situ observations. As a result, there are a great many questions as to how and why they form.

Tropical cyclones form within regions of preexisting deep, precipitating convection. Prior to cyclogenesis the convection is only loosely organized into mesoscale areas of enhanced cloudiness that are often called tropical disturbances. Only a small fraction of these tropical disturbances form tropical cyclones, and understanding why and how some disturbances undergo genesis remains elusive. Do the cyclones form quasi randomly from fortuitous interactions between mesoscale convective systems, or do predictable large-scale circulations determine the time and place of genesis?

About 80%–90% of all tropical cyclones form within 20° of the equator. This raises the possibility that tropical cyclogenesis events may be modulated by the family of equatorial and near-equatorial waves that propagate zonally in this band. The waves could cause cyclones to form by organizing deep convection and/or by altering the flow in preferred areas. It is our hypothesis that a large fraction of tropical cyclones form when tropical waves produce anomalously favorable conditions for genesis. This paper examines relationships between tropical cyclogenesis events and tropical wave activity. It focuses on the phase relationships between the waves and tropical cyclone formation. The primary goals are to improve the understanding of these relationships and to explore the potential for long-range forecasts of tropical cyclogenesis using statistical models.

Corresponding author address: W. M. Frank, Department of Meteorology, The Pennsylvania State University, 503 Walker Building, University Park, PA 16803.
E-mail: frank@ems.psu.edu

b. Conditions at the genesis location

The climatological conditions associated with tropical cyclogenesis are relatively well established. Briegel and Frank (1997) summarized seasonal studies of cyclogenesis (e.g., Gray 1968, 1979, 1985). Collectively, they show that in the current climate most tropical cyclones form in regions that exhibit four characteristics: 1) sea surface temperatures above 26.5°–27.0°C coupled with a relatively deep oceanic mixed layer; 2) cyclonic low-level relative vorticity and planetary vorticity; 3) weak to moderate (preferably easterly) vertical wind shear; and 4) organized deep convection in an area with large-scale ascending motion and high midlevel humidity. However, these characteristics are not fully independent, and they tend to be present over widespread areas of the tropical oceans much of the time. Because tropical cyclogenesis is infrequent at any one location, the conditions that cause individual storms to form must differ from the climatological conditions in nature and/or degree.

Composite analyses (e.g., McBride and Zehr 1981) and numerous observational case studies (e.g., Zehr 1992) have shown that most storms form in regions that exhibit both anticyclonic upper-level relative vorticity and cyclonic low-level vorticity in the immediate vicinity of the prestorm disturbance. Furthermore, genesis is favored in regions of weak easterly shear (supported by modeling studies beginning with Kurihara and Tuleya 1981, 1982), though there is often strong vertical shear just a few hundred kilometers away from the incipient storm location. Other case studies support the concept that tropical cyclogenesis may require the atmosphere to be preconditioned to high values of humidity in the low to midtroposphere to inhibit negative effects of downdrafts (Bister and Emanuel 1997).

While we have improved our knowledge of the conditions present at the time and place of genesis, we have less understanding of the circulations that produce them. The most common location for cyclogenesis is within or close to the intertropical convergence zone (ITCZ), particularly in the portions of the ITCZ that exhibit a monsoon trough (MT) configuration with westerly flow equatorward of the trough axis (e.g., Briegel and Frank 1997; Ritchie and Holland 1999). A MT provides an environment that satisfies all of the criteria for genesis mentioned above. Both observational studies (e.g., Ferreira and Schubert 1997) and model simulations (e.g., Wang and Frank 1999) suggest that a MT may break down spontaneously to form tropical cyclones if it remains unperturbed for a long enough period of time. However, external influences on the MT can accelerate the genesis process in preferred portions of the MT. It is probable that most storms form in conjunction with some sort of external perturbation of the trough and that pure ITCZ breakdown occurs only during times when such interactions are absent.

The ITCZ is perturbed by a variety of external circulations. For example, Briegel and Frank (1997) showed that typhoons in the northwest Pacific Ocean have a tendency to form in the ITCZ when a midlatitude trough is north-northwest of the eastern end of the MT. However, the most common modulations of the large-scale flow in the low latitudes are due to zonally propagating equatorial and near-equatorial waves. This study examines some aspects of the role of those tropical waves in the formation of tropical cyclones.

c. Tropical waves

A recent global climatology of tropical wave activity (Roundy and Frank 2004a,b, hereafter RF04) analyzed the contributions to the total variance in outgoing longwave radiation (OLR) by each of the five prominent wave types with periods of 2 days or longer. One of these is the Madden–Julian oscillation (MJO; Madden and Julian 1994). Three others are classical equatorial waves that, in idealized form, are either symmetric or antisymmetric about the equator (though in practice they are usually stronger in one hemisphere than the other). These are equatorial Rossby waves (ER), mixed Rossby–gravity waves (MRG), and Kelvin waves. The fifth wave type is confined to a single hemisphere, is westward propagating, and is known as the tropical-depression-type wave (TD type, also referred to as an easterly waves or African waves). There have been several studies of the theoretical structures of these waves (e.g., Matsuno 1966; Zhang and Webster 1989), and their observed structures (e.g., Reed et al. 1977; Hendon and Liebmann 1991; Madden and Julian 1994; Takayabu 1994; Wheeler and Kiladis 1999; Wheeler et al. 2000; Straub and Kiladis 2002; Kiladis et al. 2005).

RF04 found that the low-frequency MJO and ER waves combined to explain at least 15% of the total OLR variance between 20°N and 20°S latitude, and in some regions they explained at least 50% of the subseasonal local variance. The higher-frequency waves produced smaller percentages of the total variance in the Tropics, but in many areas, particularly in the Northern Hemisphere, they were also major contributors to the variance. Because OLR is at least a crude indicator of rainfall in the Tropics, the results of RF04 showed that the tropical waves play a major role in modulating the tropical rainfall. The circulations of these waves also modulate the large-scale wind fields.

d. Waves and cyclogenesis

The idea that waves can trigger tropical cyclogenesis is not new. It has been known for decades that about half of the hurricanes in the North Atlantic form from African waves (e.g., Frank and Clark 1980), and there have been many studies of this type of genesis (e.g., Carlson, 1969; Landsea, 1993; Thorncroft and Hodges, 2001; and others). Molinari and Vollaro (2000), Maloney and Hartmann (2001), Liebmann et al. (1994), and others have showed effects of the MJO on North Pacific tropical cyclogenesis. Dickinson and Molinari (2002) analyzed events of cyclogenesis in the northwest Pacific associated with MRG waves. Bessafi and Wheeler (2006) and Hall et al. (2001) analyzed the relationships between the MJO and ER, MRG, and Kelvin waves and genesis over the southern Indian Ocean and in the Australian region, respectively.

We propose that the zonally propagating waves in the tropical atmosphere play major roles in causing tropical cyclogenesis by enhancing local conditions in environmentally favorable areas. They can enhance the potential for genesis in several ways: by increasing upward vertical motion and convection (which also tends to lead to increased deep-layer moisture), by increasing the low-level vorticity, and/or by altering the local vertical shear pattern. Some types of waves may also trigger convection in regions of converging zonal wind, where wave energy tends to accumulate (Ritchie and Holland 1999). The larger-scale waves, such as the MJO and ER, can alter the mean zonal wind over large enough time and space scales to affect the mean flow in which the smaller and higher-frequency waves propagate. Finally, some of the lower-frequency waves might also affect sea surface temperatures sufficiently to have some effect on genesis, but this is not explored in the current study.

This paper explores the relationships between the major tropical wave types and tropical cyclone formation in each of the six major tropical cyclone basins. Satellite imagery and wind data from global analysis fields are used to determine relationships between wave activity and cyclogenesis in each region and to analyze the anomaly fields at the genesis location produced by each wave type. The data and methodology are described in section 2. The results are presented in section 3, and discussion and conclusions are presented in section 4.

2. Methodology

a. Data

The data used to isolate and analyze the wave activity and the tropical cyclones cover the years 1974–2002. The OLR data are daily means on a 2.5° grid and were obtained from the Climate Diagnostics Center. Daily wind estimates for 850 and 200 hPa were obtained from the National Centers for Environmental Prediction–National Center for Atmospheric Prediction reanalysis. The tropical storm genesis dates and locations are based on the archived best tracks of the National Oceanic and Atmospheric Administration (NOAA) Tropical Prediction Center and the U. S. Navy's Joint Typhoon Warning Center. They were obtained from Dr. Kerry Emanuel's Web site. The time at which the disturbance was first classified as a tropical depression was used as the time of genesis.

b. Spectral analysis and filtering

Figure 1 (from RF04), is a spectral analysis of the OLR data with frequency as the ordinate and wavenumber as the abscissa. Values are normalized by dividing by an estimated background spectrum (RF04; Wheeler and Kiladis 1999). Negative wavenumbers denote westward-propagating waves. Also shown in this figure are the regions of the spectral space that were assumed to correspond to the indicated wave types (outlined by heavy gray lines). These areas represent the bands over which the OLR and wind data were spectrally filtered to isolate the individual wave types. Filters applied by Wheeler and Kiladis (1999) are outlined in heavy-dashed lines for comparison. Though the spectra of the same waves may differ between OLR and winds, our filters are broad and, with the exception of the filter for the Kelvin wave, they extend to wavenumber 1 or 0 over their entire frequency ranges, allowing them to capture both the strongest OLR signals and the corresponding larger spatial scales that tend to have more power in the winds. Thin black lines in Fig. 1 indicate theoretical solutions of the shallow-water wave equations for the indicated equivalent depths. The large box in the upper left of the figure is a combined TD-type and MRG wave band. In practice it is hard to entirely separate these two higher-frequency wave types using this kind of spectral filtering because they occupy overlapping wavenumber–frequency space, but our composite analysis below makes both wave types apparent where they occur.

The spectral analysis and filtering techniques are described in detail in RF04. The OLR and wind data were spectrally filtered for each of the outlined regions shown in Fig. 1. It is important to note that just because the filter bands include the domains of the solutions of the shallow-water wave equations, not everything that passes through the bandpass filter is necessarily representative of that theoretical wave type.

The filters applied here did not include cross-

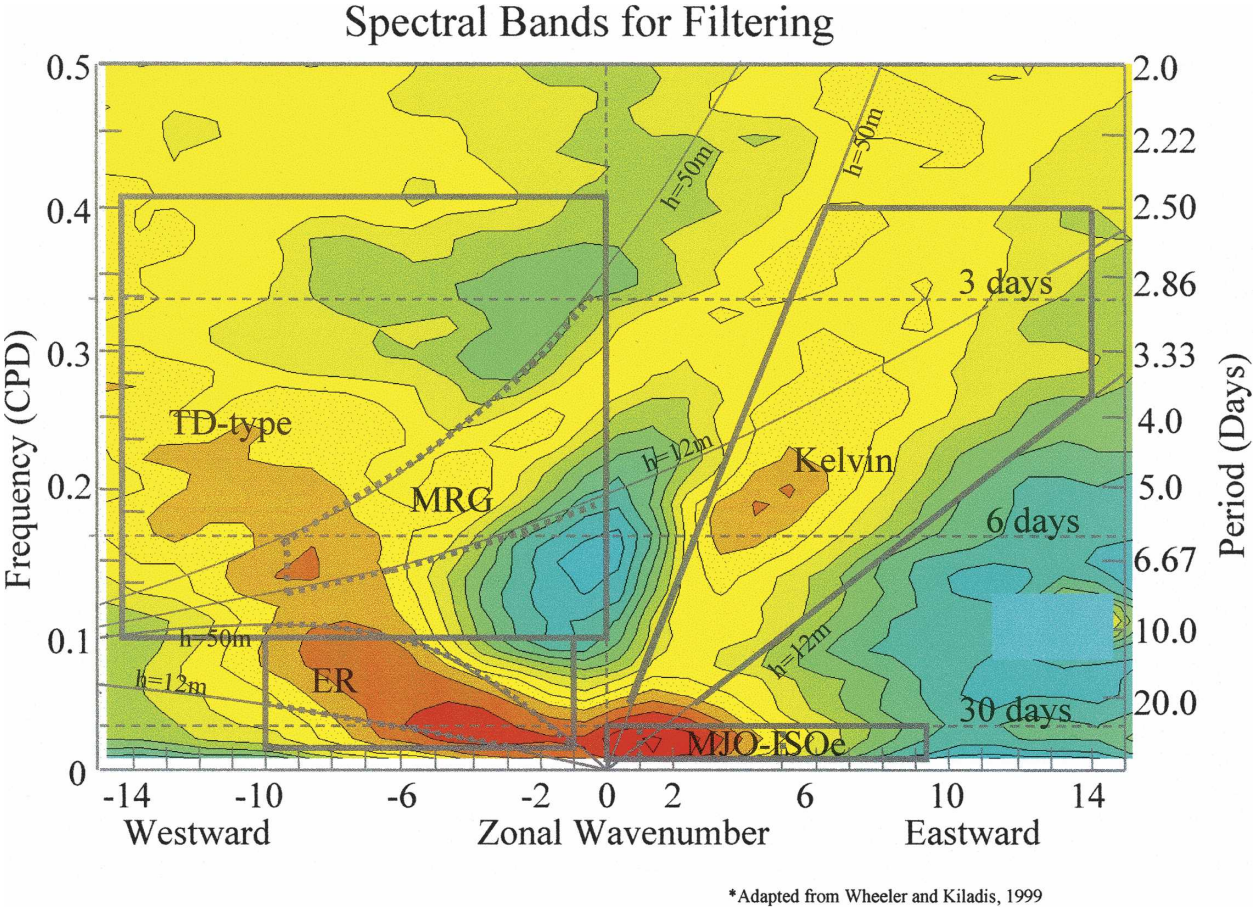

FIG. 1. Normalized wavenumber–frequency spectrum of OLR. Spectral bands of the four filters used in this project are indicated by the heavy solid lines. Bands applied by Wheeler and Kiladis (1999) are included for comparison (heavy dashed lines). Thin solid lines show the shallow-water-model solutions in a dry, motionless atmosphere for the equivalent depths indicated by the labels.

equatorial symmetry constraints. RF04 found that while all wave types are present in both hemispheres, there are major differences in the amplitude of the wave activity (Fig. 2). The MJO is by far the most active wave type in the Southern Hemisphere, while the higher-frequency waves are all much more prominent in the Northern Hemisphere. Relaxing the symmetry constraints allows the composites (discussed below) to show the natural asymmetry of the waves.

c. Composites and other analyses

The locations of the genesis events that occurred during the 29-yr period are shown by the small circles in Fig. 3. Also shown are six rectangular areas labeled 1–6. These regions were chosen as the analysis areas for the six tropical cyclone basins: 1) north Indian Ocean, 2) south Indian Ocean, 3) northwest Pacific Ocean, 4) South Pacific Ocean, 5) northeast Pacific Ocean, and 6) North Atlantic Ocean. The boxes were restricted to latitudes equatorward of 20° in order to focus on genesis cases where tropical waves would have their strongest effects. These boxes contain the majority of the genesis locations in each basin except the North Atlantic.

The amount of variance in each wave band was estimated for each genesis event at the location and date of genesis. Genesis events were classified as to whether or not they occurred when waves were active within that basin. Time series of variance were estimated for each grid point by smoothing the squared filtered anomaly with a running mean in time. The windows for the running means were 51 days for the MJO, 21 days for the ER band, and 11 days for both the MRG–TD-type and Kelvin bands (somewhat longer than the dominant period in each of these bands). A wave band was considered active when its OLR variance was locally above a threshold value (see the appendix). Note that though wave dynamics controls much of the variability of individual wave types, variability in one filter band is not necessarily independent from variability in the other bands and in tropical cyclones, as activity of each of

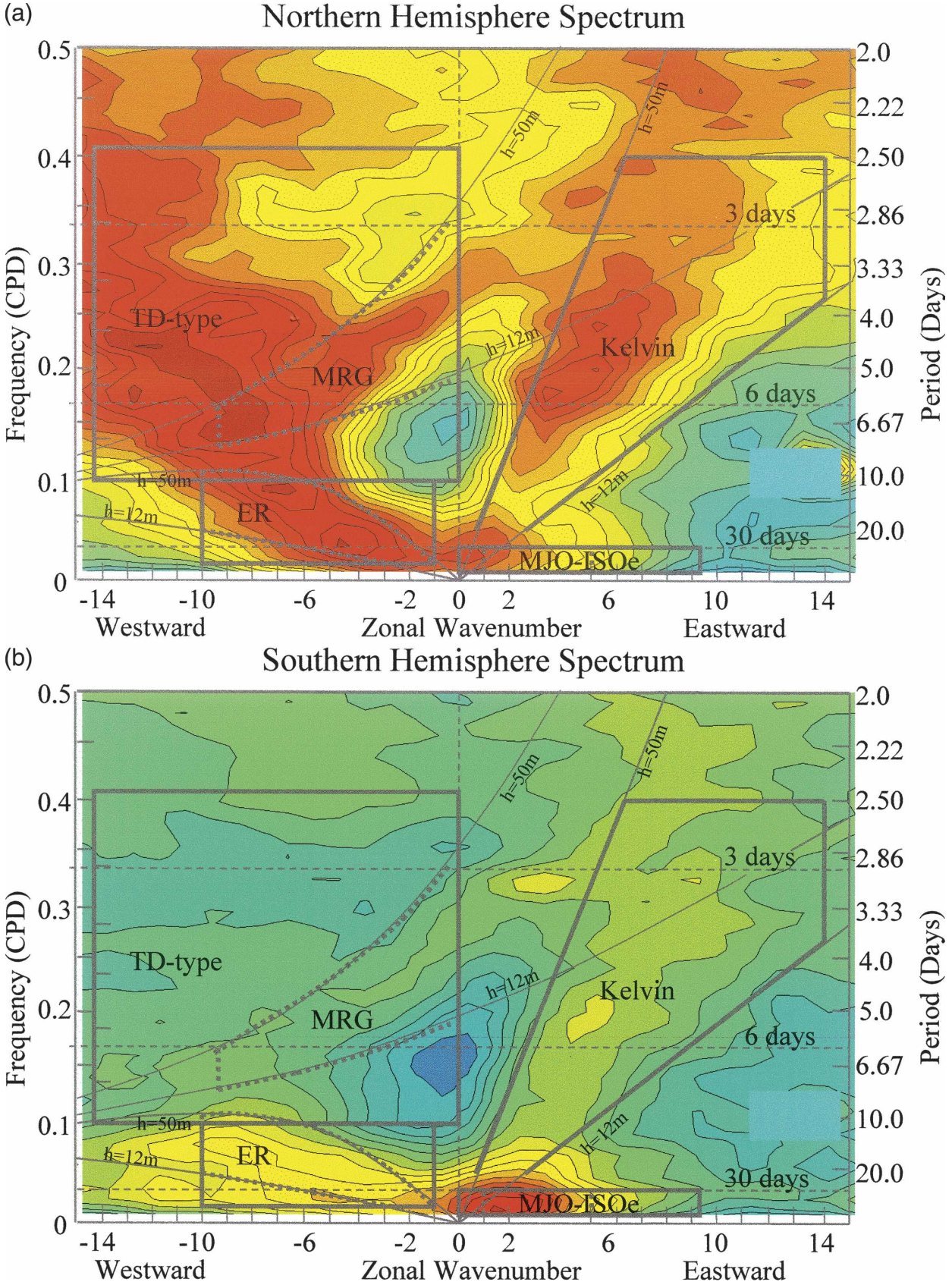

FIG. 2. Same as in Fig. 1, but for the Northern and Southern Hemispheres separately.

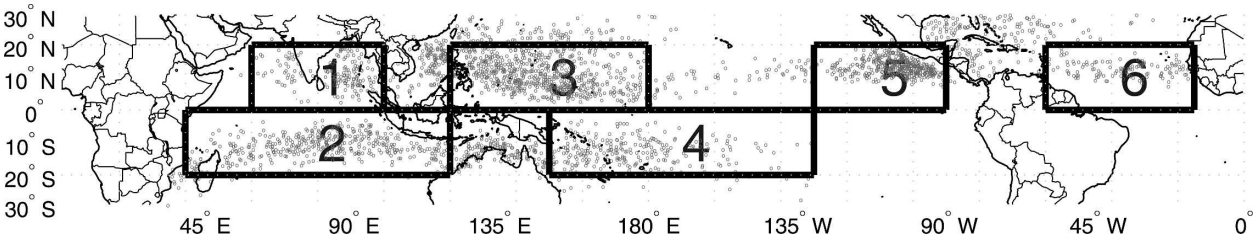

FIG. 3. The rectangular boxes show the six cyclone basins defined for this study, and the individual dots show genesis locations for the individual storms for the period 1974–2002.

these may vary with the activity of total OLR. Each genesis event was classified as to whether it occurred in the positive or negative OLR anomaly region of each wave type.

Composites of total unfiltered OLR, OLR anomalies, and the 850- and 200-hPa wind anomalies were each constructed relative to the genesis point and time lags from the genesis date for each spectral band in each basin. These composites included only those genesis events that occurred during periods when the filter band of interest was locally active at the genesis point (by using the threshold discussed in the appendix). The composite structures were compared with theoretical wave structures and were used to determine the phase relationships between genesis and wave activity. The Kelvin wave analysis was limited to storms forming equatorward of 10°N and 10°S, because Kelvin wave activity tends to be more concentrated near the equator than the other wave types.

Time–longitude composite diagrams were constructed for each filter band and region relative to the genesis point. These were used to determine whether the wave anomaly could be detected propagating into and out of the genesis location.

A 1000-sample bootstrap significance test was applied to the composite OLR and wind anomalies, assuming the null hypothesis that the anomalies were not significantly different from zero. This was done by randomly selecting (with replacement) from the set of genesis dates included in the composite, applying the averaging to each new set, and locating the zero anomaly within the resulting distribution.

3. Results

a. Seasonal variations of wave activity and genesis

A useful climatological question is the following: How do the annual cycles of variance in each wave band compare with the annual cycles of genesis in each basin? Each of the six tropical cyclone basins has its own unique climatology. Therefore, a first step is to determine whether the cyclone season coincides with the mean seasonal wave activity within the region. Each panel of Fig. 4 shows the mean annual cycles of wave-filtered OLR variance and tropical cyclogenesis within the rectangular analysis area of the indicated basin. In each panel the heavy black line is an index of the number of tropical cyclones per month that form within the box. The OLR variance shown in the other lines is just the square of the filtered anomalies averaged over the basin and the day of the year.

An important caveat is that in some cases waves may impact tropical cyclone formation without producing significant effects upon the OLR pattern, such as by altering the vertical shear and/or increasing the low-level vorticity. Examples of this include the roles of the MJO in genesis in the northeast Pacific and the North Atlantic (discussed below).

In the Southern Hemisphere the results are straightforward. The annual cycles of OLR variance in the MJO and ER bands tend to vary in phase with the cyclone season. The MRG–TD wave activity is in phase with the cyclone season, but the cyclones themselves might be contributing a significant part of the signal. Kelvin wave activity in the South Indian Ocean clearly varies in phase with the cyclone season, and this pattern is similar but less distinct in the South Pacific.

The patterns are much more variable in the Northern Hemisphere basins. The cyclone season of the north Indian Ocean basin differs from the other basins in that the monsoon trough spends most of the late summer over land and relatively far north of the equator. Hence, it has two distinct genesis peaks in the spring and autumn. In this basin the first peak coincides with peaks in MJO, ER, and Kelvin band activity. None of these wave types is particularly active during the second peak of the cyclone season. The MRG–TD-type and ER bands have sharp peaks in activity during the middle and late summer, but these do not coincide with either cyclone peak.

The northeast Pacific shows only weak seasonal relationships between wave activity and cyclone forma-

tion. The MRG–TD-type waves are somewhat more active during cyclone season than in the other months and Kelvin waves remain active during the earliest part of the cyclone season. The northwest Pacific shows strong annual cycles in MRG–TD-type and ER wave activity that coincides well with the cyclone season. The other wave types do not vary in phase with the cyclone season. In the North Atlantic the MRG–TD-type waves vary roughly in phase with the cyclone season, while the other three wave types do not.

Comparing Figs. 2 and 4 it is clear that the low-frequency MJO band and ER band variances that dominate the Southern Hemisphere spectrum are strongly seasonal, and they vary in phase with the cyclone season in the two Southern Ocean basins and for the first peak of the North Indian season. Activity in the Kelvin band tends to follow the same pattern, though the cycles are somewhat less distinct than for the MJO and ER bands.

All of the wave types (except the MJO) are more active in the Northern than in the Southern Hemisphere. This is particularly true for the MRG–TD-type band, which varies strongly and in phase with the cyclone season in the North Atlantic and the northwest Pacific.

b. Individual genesis events and local wave activity

Figure 4 suggests that there are seasonal relationships between basin mean wave activity and cyclone formation in each basin, but these relationships could be coincidental. The waves might be active away from the genesis points, and they do not necessarily show all periods of wave activity, because these are not always locked to the seasonal cycle. Therefore, it is important to examine the level of local wave activity at the time of each individual genesis event. As noted above, tropical cyclogenesis is affected by circulations that occur over a broad range of scales, but it is the conditions within a few hundred kilometers of the storm center that are thought to be crucial in determining which disturbances will form cyclones. This section examines the structures of the waves that are present when tropical cyclones form and the locations of the forming storms within the wave circulation. The goal is to infer what types of flow perturbations promote genesis.

In Figs. 5a–l, the open (or white) vertical bars show the percentage of the total number of cyclones in that basin that formed when the OLR variance exceeded the threshold for each wave type. The shaded bar shows the percentage of the days when the threshold was exceeded for that wave type. The data in Figs. 5a–f are for the entire season, while the data in Figs. 5g–l are for the warm season only, which approximates the hurricane season in most basins except the North Indian. The warm season is defined here as June–October in the Northern Hemisphere and December–April in the Southern Hemisphere. When the open bar is taller than the shaded bar, it means that more storms formed when that wave type was active than would be expected if the storms formed at random times during the year (Figs. 5a–f) or during the warm season only (Figs. 5g–l). When the open bar is shorter than the shaded bar, it shows up as a line partway up the shaded bar. In this latter case, fewer storms formed when the OLR variance was above the threshold than would have been expected by chance.

Figures 5a–f show that in general storms tend to form more often when the MJO, ER, and MRG–TD-type waves are active than would be explained if the storms occurred randomly throughout the year. The exception is for the MJO band in the Atlantic. Kelvin waves do not show this tendency except in the South Indian Ocean (for a more detailed analysis, see Bessafi and Wheeler 2006). However, the apparent relationships between active waves and genesis could simply be because the waves and cyclones have similar seasonal cycles in some basins, as noted above. Hence, Figs. 5g–l, which are comparing events only in the warm seasons, are generally better indicators of possible relationships between genesis and anomalous wave activity in the region.

The warm-season results in Fig. 5 indicate that cyclogenesis is clearly related to above-normal wave activity in the MJO, ER, and MRG–TD-type bands in the northeast Pacific basin and to a lesser extent the north Indian basin. The Atlantic basin shows such relationships for the ER and MRG–TD-type bands but not the MJO. In contrast, the northwest Pacific shows no such relationship for any wave band, and the two Southern Hemisphere basins show only a weak relationship for the single MRG–TD-type band. Genesis does not appear to be associated with above-normal warm-season Kelvin wave activity in any basin, and Fig. 4 suggests that these waves would most impact genesis during northern spring. Although these results suggest that in many cases (e.g., the MJO in the northwest Pacific) waves may not tend to be more active than normal when genesis occurs, our further analysis (discussed below) suggests that they still influence genesis.

Figures 6a–f show, for each of the four major wave bands, the fraction of the cyclones that form within the negative OLR anomaly of that band. For each filtered dataset the positive and negative areas are nearly equal in size (each covering 50% of the area in space and time, typically $\pm 1\%$–2%). Therefore, a shaded bar with a value greater than 50% means that storms formed

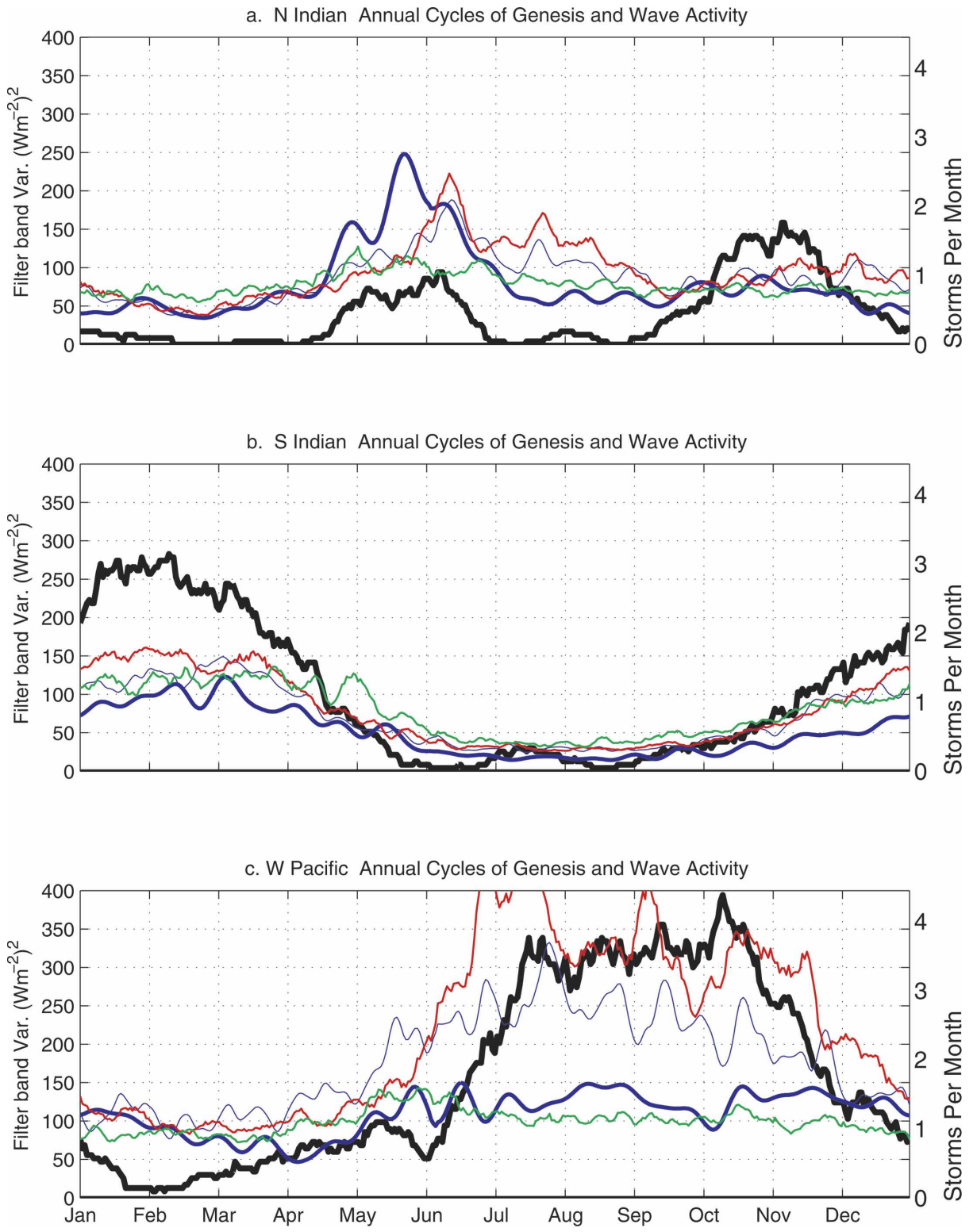

FIG. 4. Mean annual cycles of storm genesis (storms per month) and of OLR variance in the indicated filter bands for each of the six cyclone basins. The line colors are as follows: cycle of cyclogenesis (black); MJO (heavy blue); ER (thin blue); MRG–TD type (red); and Kelvin (green). Variance values are the squared filtered OLR anomalies averaged over the day of the year and smoothed for plotting with a 5-day running mean.

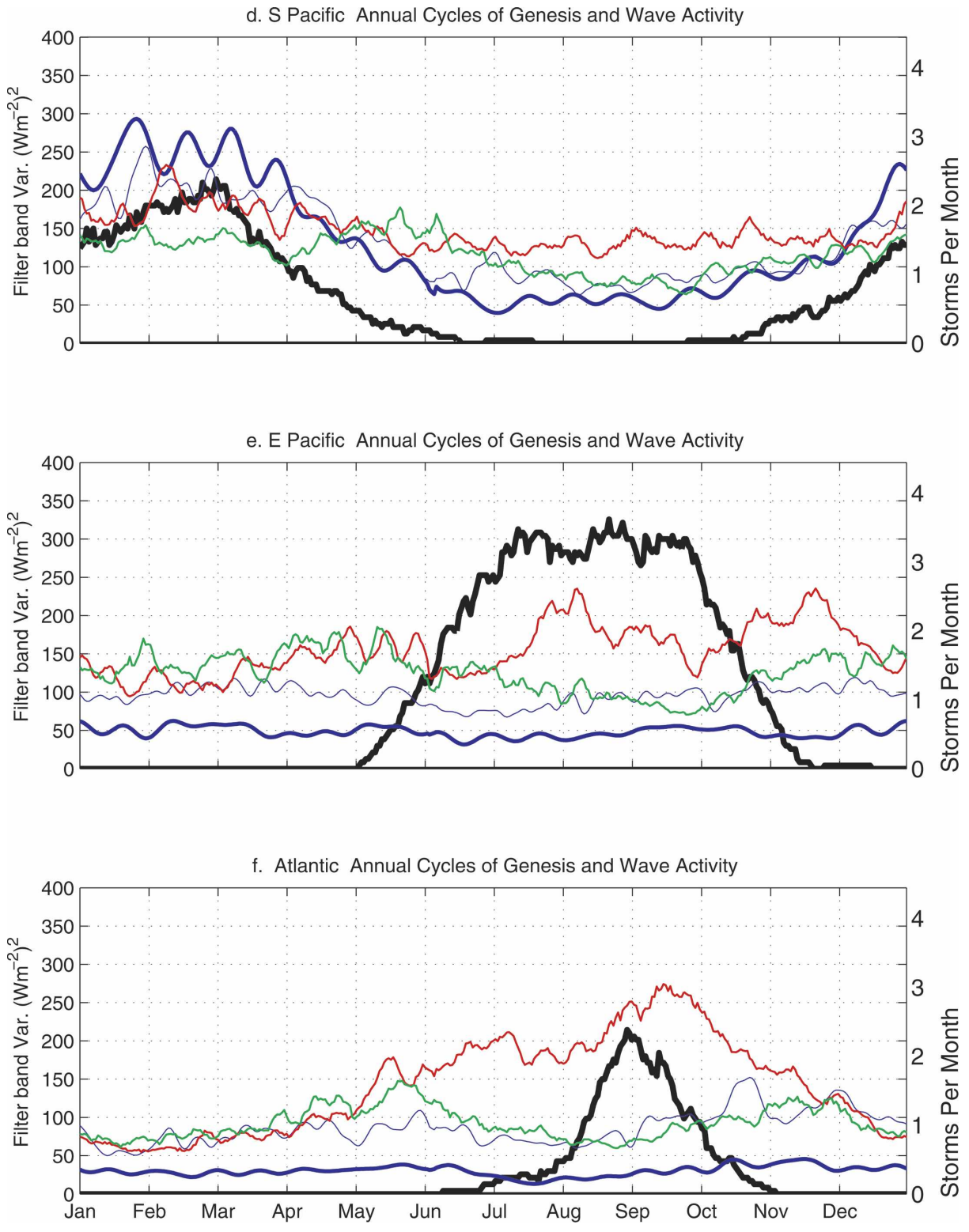

FIG. 4. (*Continued*)

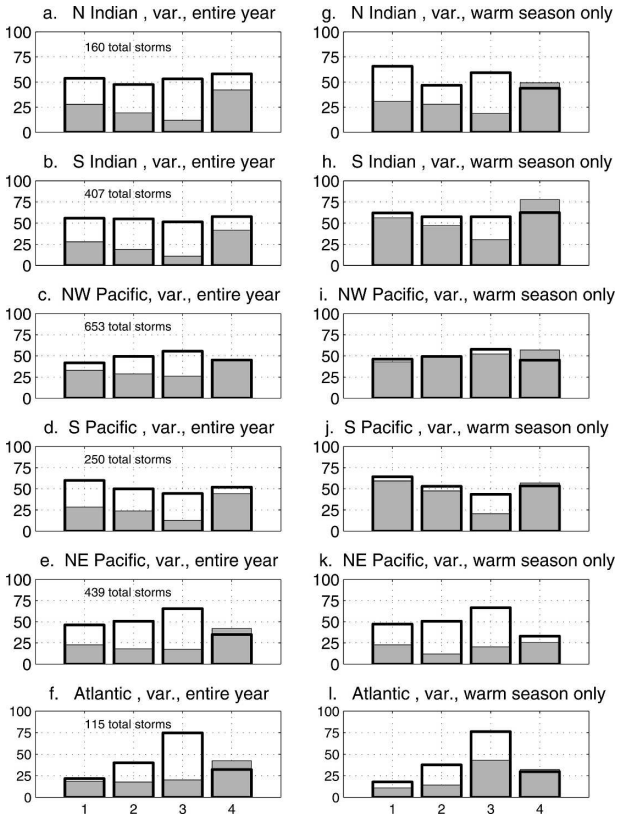

FIG. 5. For each basin and wave band the shaded bar is the percent of time that the wave variance is above the threshold value for that basin, while the open (white) bar is percentage of the genesis events that occurred when the wave variance was above the threshold. The filter-band numbers are 1 (MJO), 2 (ER), 3 (MRG–TD-type), and 4 (Kelvin). (a)–(f) Computed for the entire cyclone season, and (g)–(l) for the warm season only (see text for definitions of the warm seasons).

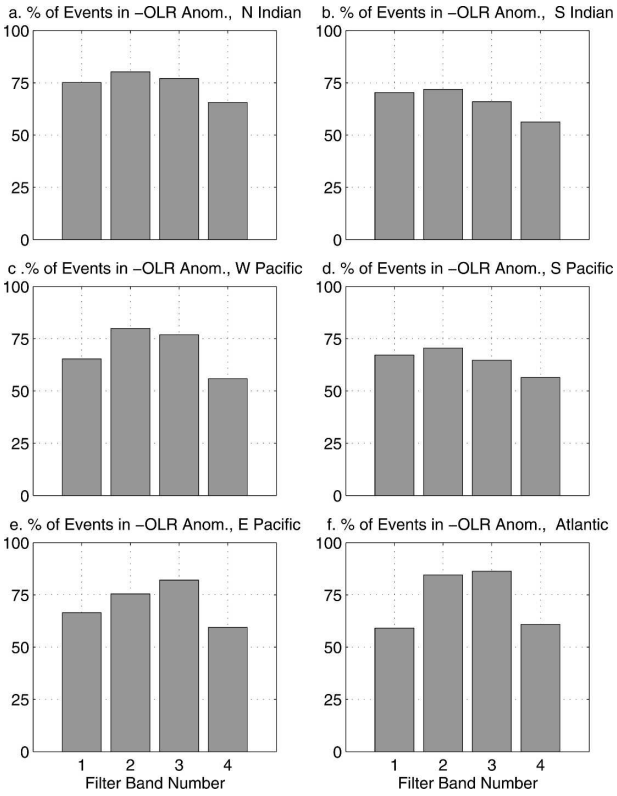

FIG. 6. For each basin and filter band, the percentage of the storms that formed within the negative OLR anomaly region for that filter band. Filter bands are numbered as in Fig. 5.

preferentially in the negative OLR anomaly region of that wave band. Because negative OLR anomalies are associated with the more convectively active portions of the waves, this represents a tendency for storms to form where waves are enhancing the convection above background values.

In all six basins the storms form in the negative OLR anomalies of the MJO band between about 60%–70% of the time, and these results are significantly different from the 50% line at the 99% level (97% for the Atlantic) using a bootstrap test. Storms also have a clear tendency to form in the negative OLR anomaly regions of ER waves in all basins. For ER waves the departures from the 50% line are all significant at the 99% level. Maloney and Hartmann (2001) suggest that the MJO influences east Pacific cyclogenesis through far-field effects, meaning that the strongest active convection of the MJO is not in the east Pacific when genesis occurs. Our method successfully diagnoses the MJO impacts in such regions, because even though the strongest MJO convection is elsewhere, MJO-band convection is still locally enhanced at the time and place of genesis during many of the events in which it plays a role. Although these results suggest that some wave types may only exceed the variance threshold during less than half of all the storm formations in some basins, our composites (below) suggest that many of these waves still show clear relationships to genesis when the waves are active.

The MRG–TD-type combined wave band also shows a clear tendency for storms to form in the negative OLR anomaly regions, with percentages ranging from a low of about 65% in the South Pacific to a high of around 85% in the Atlantic. Departures are significant at better than the 99% level in all basins. The only two basins with percentages below 75% are in the Southern Hemisphere, where this wave band is least active. Interpretation of these results is complicated because a portion of the signals of the storms themselves fall into this band.

Storms show a small preference for forming in the negative anomalies of the Kelvin wave band in all basins. Although the percentages of storms that do so are

only 55%–65%, the departures from 50% are significant at the 97% level or above.

c. Composite wave structures at genesis

In general, the composites for each wave type show similar structures in each basin. Recall that the composites are performed only for times when wave activity was above the threshold. For brevity, this discussion focuses on composites from the 850-hPa level and for the northwest and northeast Pacific basins and from the 200-hPa level for the northwest Pacific only. Results for the other basins are summarized and compared with the composites for these regions. We also performed null-case composites for each basin by compositing relative to the same genesis locations and days of the year, but for years with no tropical cyclone present. These null cases showed only a relatively smooth background reflecting the mean flow of the region with no evidence of anomalous OLR, vorticity, or other flow patterns. This result suggests that when our genesis-centered composites show clear wave structures, they provide evidence of preferred phase relationships to genesis.

Figure 7 shows the composites for the northwest Pacific at the time of genesis. In each of these figures the grid has been shifted zonally for each case so that 0° longitude is the mean longitude of the storm genesis locations. However, the grid is not shifted meridionally, so 0° on the vertical axis is the latitude of the equator. The reason for not shifting the grid meridionally is that some of the wave types maintain a close alignment with the equator and are somewhat less distinct when the grid is shifted north–south and data are then composited relative to the storm genesis point. A small open circle is plotted at the mean location of the storm genesis points, and for the northwest Pacific this is at 0° relative longitude and about 11°N actual latitude. The shaded contours show the background OLR pattern, which suggests that the mean genesis location is at the eastern edge of the monsoon trough portion of the ITCZ. This has been shown to be a favored location for genesis by Briegel and Frank (1997), Briegel (2002), Ritchie and Holland (1999), and others. The heavy black solid and dashed lines represent the band-filtered OLR negative and positive anomalies, respectively, for the appropriate wave type. The vectors show the anomalous winds for that filter band.

The northwest Pacific MJO composite shows a wind structure resembling a large Kelvin wave with westerly winds along the equator (Fig. 7a). Typhoons in this region tend to form near the easternmost edge of the low-level westerly wind surge and within the eastern and equatorward side of a cyclonic gyre, just north of the latitude of maximum anomalous westerly flow. The storms form well within the negative OLR anomaly of the MJO, indicated by the heavy, solid contours. Hence, the storms are forming in a region of MJO-induced low-level zonal confluence and convergence as well as MJO-enhanced convection. They are also forming at the time when this favorable, anomalous westerly flow region reaches the eastern edge of the monsoon trough, which is a region of strong, persistent convection and low-level cyclonic vertical vorticity. This location in the background flow is sometimes referred to as the confluence point due to the change in direction from monsoonal westerlies (to the west) to trade easterlies (to the east) on the equatorward side of the ITCZ (e.g., Briegel and Frank 1997). This confluence point is thought to be a region favorable for zonal wave energy accumulation (Briegel and Frank 1997; Ritchie and Holland 1999). Because the genesis location lies near the northern boundary of the westerly surge, the wave is also increasing the vorticity at that point.

The wind anomalies for the ER band in the northwest Pacific show a classic ER wave pattern in the Northern Hemisphere. There is a strong cyclonic gyre centered just northwest of the genesis location. The anomalous flow in the Southern Hemisphere is weak by comparison. The cyclonic gyre is located about one-quarter wavelength to the west of the center of the negative OLR anomaly. The preferred region of genesis with respect to ER waves is within the region of large-scale cyclonic flow of the wave anomaly and is also within the negative OLR anomaly region (Fig. 7b). The anomalous rotational flow of the ER wave reinforces the vorticity of the monsoon trough. Furthermore, the storm forms during the time that the wave-enhanced convection reaches the confluence point of the ITCZ.

For the MRG–TD-type band the pattern is similar and is shown in Fig. 7c. The structure near the genesis location shows a wave propagating toward the west-northwest (confirmed by analysis of lag composites, not shown). In this band the wave anomaly circulation indicates that the genesis location occurs within the western edge of the low-level cyclonic circulation associated with the wave and in northeasterly anomalous flow. It also forms within the region of negative OLR anomaly. Dickinson and Molinari (2002) analyzed cases of MRG waves in the northwest Pacific moving toward the northwest and transforming into TD-type waves after they reach the monsoon trough. The composites support their conclusions and suggest that this movement off the equator generally occurs at or about the time of genesis when the MRG–TD-type disturbances reach the confluence point of the ITCZ. Their case study in-

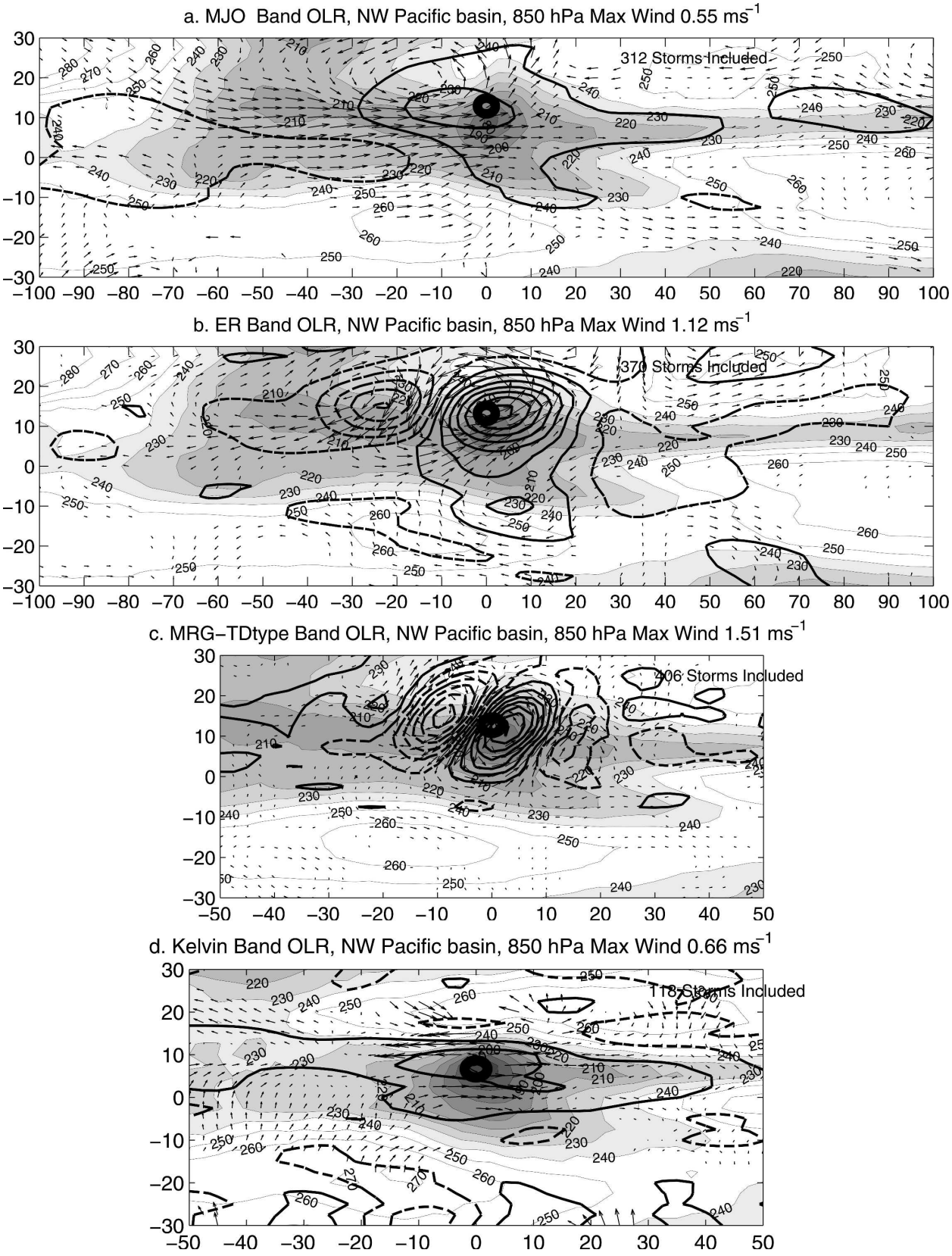
a. MJO Band OLR, NW Pacific basin, 850 hPa Max Wind 0.55 ms^{-1}
312 Storms Included
b. ER Band OLR, NW Pacific basin, 850 hPa Max Wind 1.12 ms^{-1}
370 Storms Included
c. MRG–TDtype Band OLR, NW Pacific basin, 850 hPa Max Wind 1.51 ms^{-1}
406 Storms Included
d. Kelvin Band OLR, NW Pacific basin, 850 hPa Max Wind 0.66 ms^{-1}
118 Storms Included

cluded three different genesis events that each occurred in somewhat different flow patterns. Our composite result suggests that the preferred genesis point in an MRG wave train is in anomalous northeasterly 850-hPa flow within counterclockwise gyres as the waves move off the equator. Case 3 in Fig. 6m of Dickinson and Molinari (2002) is most similar to the composite behavior.

The Kelvin wave–band composite (Fig. 7d) suggests a relationship between cyclogenesis and Kelvin-band OLR anomalies, but the relationship is less clear in the wind data because the classic Kelvin wave structure is hard to discern. (There is some evidence of a Kelvin wavelike westerly surge at 850 hPa near and east of the genesis point, but there is also an easterly surge north and west of the genesis point.) Kelvin wave structures are not clearly discernable in the winds in any basin, but this does not necessarily mean that Kelvin waves never affect genesis—some storms that develop close to the equator, especially in the Pacific ITCZ during the northern spring or in the Indian Ocean during the southern summer, might be impacted by them. We have seen relatively rare cases in which Kelvin waves might have influenced genesis in the northeast Pacific during May, including Hurricane Adrian during May 2005. This needs further investigation, but it is clear that such events are not frequent enough to produce a strong signal in the statistics.

Figures 8a–d shows the same four composites for genesis in the northeast Pacific. The results are qualitatively similar. The shaded background OLR fields indicate that genesis in this region tends to occur within the western part of the monsoon trough. Storms tend to form near the eastern edge of the westerly wind anomaly and within the negative OLR anomaly of the MJO. As in the northwest Pacific, the genesis location is at the poleward edge of the MJO westerly anomaly, so the wind surge is increasing the low-level rotation as well as the convergence at this location. For the ER band the storms form within the cyclonic rotation of the ER wave (southeast of the center of rotation) and within the negative OLR anomaly. They also form within the low-level cyclonic rotation of the MRG–TD-type waves and the region of the negative (enhanced convection) OLR anomaly. Once again, the Kelvin wave band shows slightly enhanced convection (negative OLR anomaly) at the time and place of cyclogenesis, but there is no clear sign of a Kelvin wave in the composite wind structure.

The composites for the remaining four basins are qualitatively similar to those for the northwest and northeast Pacific with the following exceptions.

In the south Indian and South Pacific basins the cyclones tend to form within, rather than at the eastern edge, of the westerly flow of the MJO. (The MJO anomalous flow in the south Indian basin is west-northwesterly.) In the Atlantic genesis occurs within an MJO westerly flow anomaly that is concentrated in the vicinity of the ITCZ within a small negative OLR anomaly.

MRG–TD-type anomalies are weaker and less distinct in the two Southern Hemisphere basins than they are in the four Northern Hemisphere ones. This is particularly true in the South Pacific. However, they do show similar structures and phase relationships to those in the Northern Hemisphere. The lagged composite structures suggest that MRG waves may occasionally influence cyclogenesis in the Indian basin, in a manner similar to that discussed above in the northwest Pacific (e.g., Dickinson and Molinari 2002).

The upper-level composites for the MJO, ER, and MRG–TD-type bands in the northwest Pacific are shown in Fig. 9. Results for the northeast Pacific are generally similar (not shown). Many of the upper-level composites show wave structures more clearly than those at 850 hPa. For example, Fig. 9b shows anticyclonic and cross-equatorial outflow from the developing storm being integrated into a wind pattern that is symmetric across the equator suggestive of an $n = 1$ ER wave, where n is the meridional wavenumber. Comparing the 200- and 850-hPa composite anomalies for each wave type shows that the upper-level winds are roughly opposite in direction to the low-level winds suggesting that each of these wave anomalies is dominated by a baroclinic, first internal mode vertical structure for the portions of the wave near the genesis location. This tendency for the upper- and lower-level winds to be in opposite directions is generally true in the other four basins as well, with the lone exception being the MRG–TD-type waves in the South Pacific basin, where the

←

FIG. 7. Composite of the OLR anomalies (contours), 850-mb wind anomalies, and total OLR (shading) relative to the genesis point and date in the NW Pacific for (a) MJO, (b) ER, (c) MRG–TD-type, and (d) Kelvin filter bands. The contour interval for OLR anomalies is 2 W m^{-2}, with minimum contours at ± 1 W m^{-2}. For all wave types except the Kelvin wave, the first contour is significantly different from zero at >95% level, and the second contour exceeds the 99% level. For the Kelvin wave, the second contour generally exceeds the 95% level. Wind anomaly vectors are plotted only when they exceed the 90% level for a difference from zero.

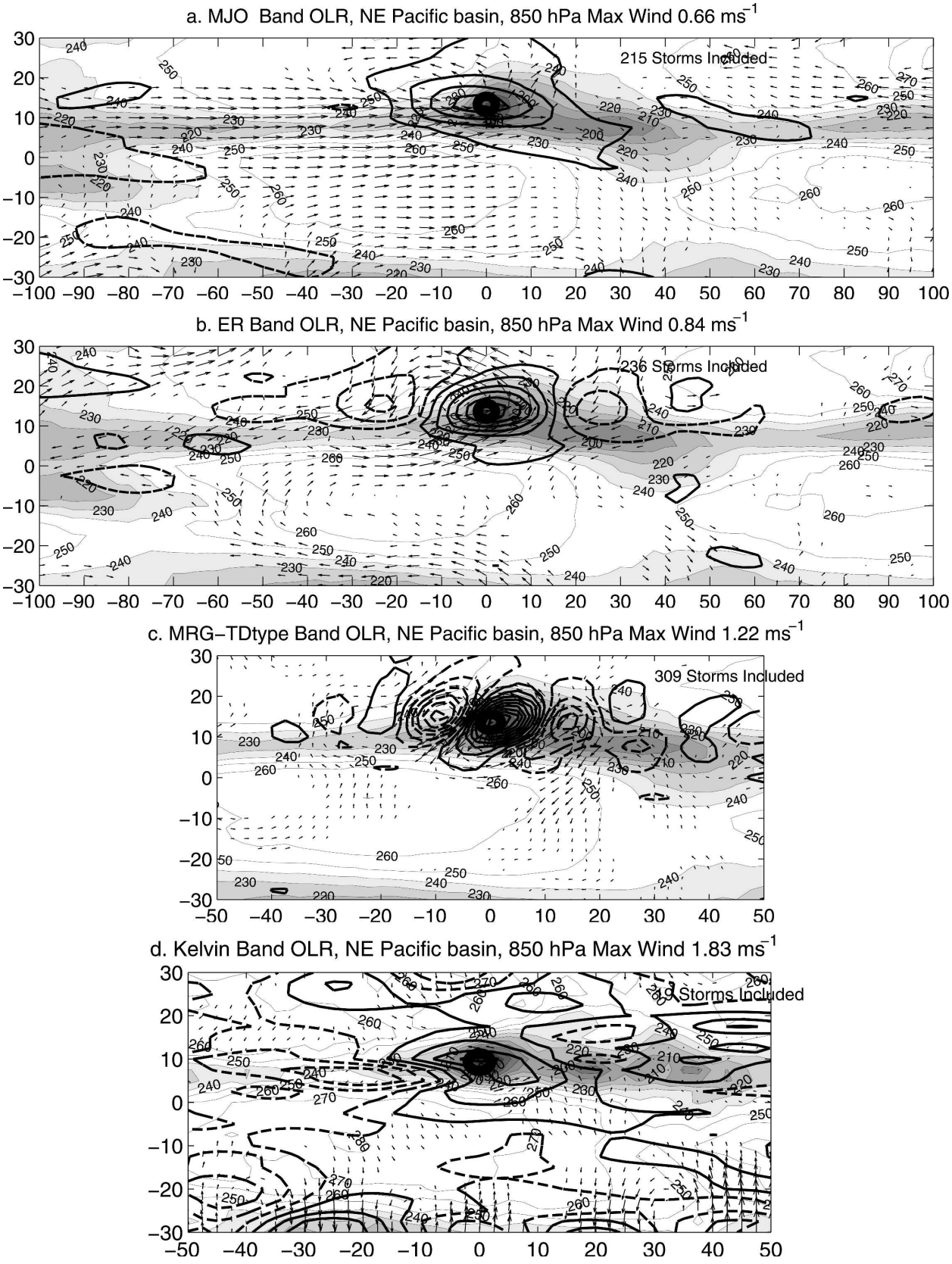

FIG. 8. Same as in Fig. 7, but for the northeast Pacific.

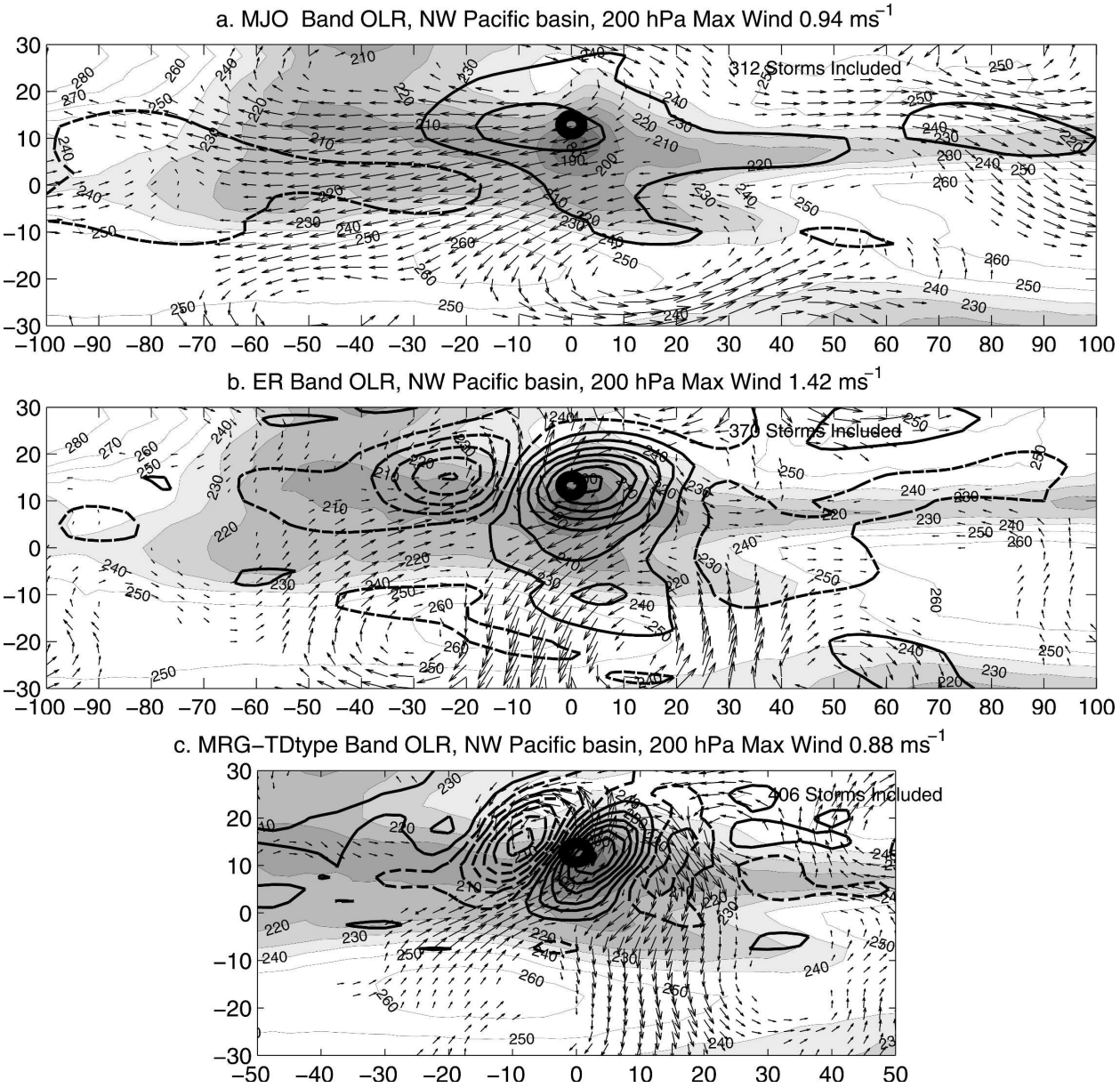

FIG. 9. Same as in Fig. 7, but with the 200-mb winds in the northwest Pacific. The Kelvin wave band is not shown.

anomalous wind patterns are indistinct in this band. The commonly observed first internal mode vertical structure would allow the waves to modulate vertical shear in a manner that might influence genesis. For example, the climatological mean 850–200-hPa vertical shear of the zonal wind averaged over 5°–12.5°N is westerly over the Atlantic between 40° and 70°W for July–September. Shear of the composite MJO flow over the central tropical Atlantic near the genesis point (not shown), is easterly and significantly different from zero. This shows that the MJO often reduces the total westerly shear over the Atlantic when genesis occurs.

The southwesterly vertical shear of composite MRG–TD-type winds is significantly different from zero in the northwest and northeast Pacific and Atlantic basins. Within the limits of the current analysis, there do not appear to be significant anomalies in the vertical shear associated with the Kelvin wave. The MJO band shows genesis occurring in a region of significantly enhanced easterly shear in all basins except the north Indian, while in the ER band there are significant easterly shear anomalies in the north Indian, south Indian, northwest Pacific, and perhaps the northeast Pacific basins but none in the South Pacific or Atlantic. Wave-

induced shear anomalies may enhance genesis by reducing the total shear in regions where the background shear is inhibitive.

Altogether, the composites portray clear and relatively consistent phase relationships between tropical cyclogenesis and tropical wave activity. For example, northwest Pacific typhoons tend to form within the cyclonic anomalies associated with the MJO, ER, and MRG–TD-type waves. This suggests that the waves enhance the tendency for genesis in part by increasing the local low-level vorticity. Because storms are observed to form within the convectively active portions of these waves, the results suggest that large-scale enhancement of deep convection enhances storm genesis. The MJO and ER waves also produce an easterly shear anomaly at the genesis location.

d. Timing of wave-induced genesis

Time–longitude diagrams were computed for the OLR anomalies in each filter band and for each basin. The OLR anomalies were plotted at the mean latitude of genesis events that occurred when the wave band of interest was active. These diagrams were used to estimate how long before genesis the wave anomalies could be detected. If a wave is detectable several days before genesis occurs, it implies that forecasts of tropical cyclogenesis based on wave projections should be feasible. By detectible, we mean that the composite OLR anomalies are significantly different from zero at the 99% level. Figure 10 shows these diagrams for the MJO, ER, MRG–TD-type, and Kelvin bands in the northwest Pacific. Figure 11 shows the diagrams for the first three of these bands in the northeast Pacific.

The significant eastward-moving negative OLR anomalies of the MJO reached the genesis location from 5 days (south Indian) to 15 days (northwest Pacific) prior to the time of genesis in all basins, except in the Atlantic. In the Atlantic, the negative anomaly at the genesis point exceeded the 95% level about 5 days prior to genesis. In each of the basins the negative OLR anomalies become significant to the west of the genesis location much earlier—17 days prior to genesis in the northwest Pacific and 18 to more than 30 days in the other basins. These precursor anomalies first become significant 45°W of the genesis point in the north Indian and northwest Pacific, 50°W in the south Indian and northeast Pacific, 100°W in the northeast Pacific, and 40°W in the North Atlantic.

The negative OLR anomalies in the ER band arrive at the genesis location one to two days prior to the time of genesis in all six basins. These westward-moving anomalies first become significant in the composites at the 99% confidence level about 4 days prior to and 20°E of the genesis point in the north and south Indian Ocean, 5 days prior and 30°E in the South Pacific and Atlantic, 8 days prior and 35°–40°E in the northwest Pacific, and 15 days prior and 100°E in the northeast Pacific.

In the higher-frequency MRG–TD-type band the negative OLR anomaly associated with genesis tends to become significant to the east of the genesis point from 3–6 days prior to the formation of the storm, with the longest lead time being in the northeast Pacific. Genesis occurs very soon after the negative OLR anomaly becomes significant at the genesis point (0–1 days). The signal is stronger in the Northern Hemisphere, which was expected because these waves are much stronger in general there.

Kelvin-band Hovmoellers suggest significant negative OLR anomalies 3–7 days prior to genesis in most basins. The anomalies are less clear than in the other bands, but they tend to arrive at the longitude of the genesis location on the day of or the day after genesis.

4. Summary and discussion

The results show that three classes of equatorial waves play significant roles in the formation of many of the 80 or so tropical cyclones that form each year within the six major cyclone basins. These wave types include the MJO, equatorial Rossby waves, and high-frequency westward-moving waves including mixed Rossby–gravity waves and tropical-depression-type disturbances. Equatorial Kelvin waves do not appear to play a major role in tropical cyclogenesis, except in isolated events, especially during the Northern Hemisphere spring or during the southern summer in the southern Indian Ocean (Bessafi and Wheeler 2006). The remainder of this discussion will consider only the first three wave bands.

Analyses of the seasonal variations of wave activity and cyclogenesis in the six global cyclone basins shows interesting variations from region to region, but they provide only suggestions of relationships between the waves and genesis. Some regions have cyclone seasons that vary in phase with different types of waves, while others show less seasonal variation in wave activity.

When basin-scale wave activity is computed at the times of genesis events, clearer patterns emerge. In two Northern Hemisphere basins (e.g., the north Indian and northeast Pacific) there is a distinct tendency for genesis to occur more often when wave variance in any of the three filter bands is above the threshold (see the appendix). In the North Atlantic the same pattern is seen for the ER and MRG–TD-type bands. The relationship of the MJO to genesis in the North Atlantic is

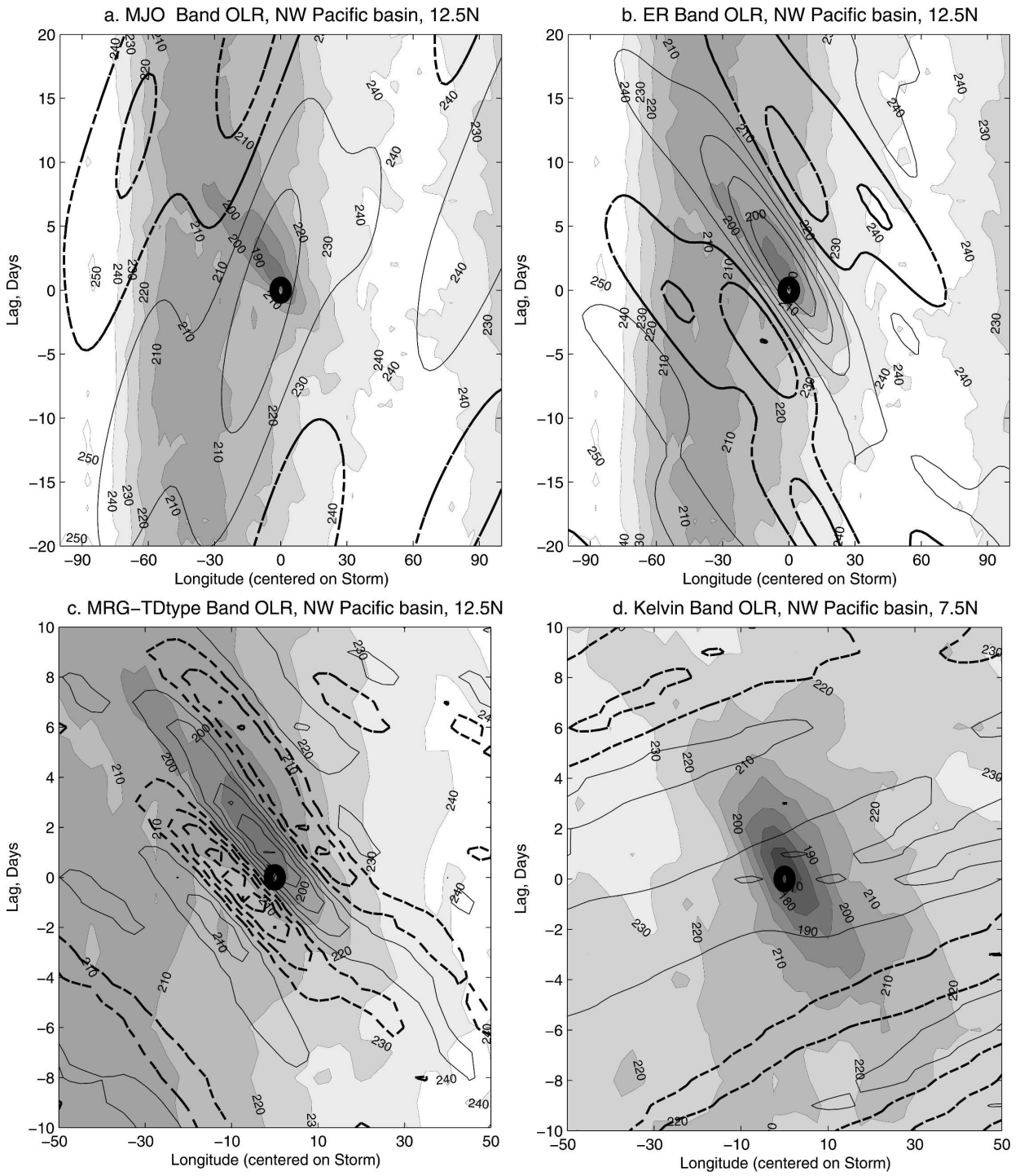

FIG. 10. Composite Hovmoeller diagrams of OLR anomalies in the northwest Pacific for (a) MJO, (b) ER, (c) MRG–TD-type, and (d) Kelvin filter bands. The contour interval is 2 W m^{-2}, with minimum contours at ±1 W m^{-2}. The confidence levels for the difference from zero are approximately the same as those given in Fig. 7.

more complicated because only about one-quarter of the storms that form there do so when the MJO band is considered locally active in OLR. The composites suggest that these storms may be more strongly influenced by far-field effects of the MJO than by its small contribution to local convection, as suggested by Maloney and Hartmann (2001) in relation to genesis in the east Pacific. In contrast to the other three Northern Hemi-

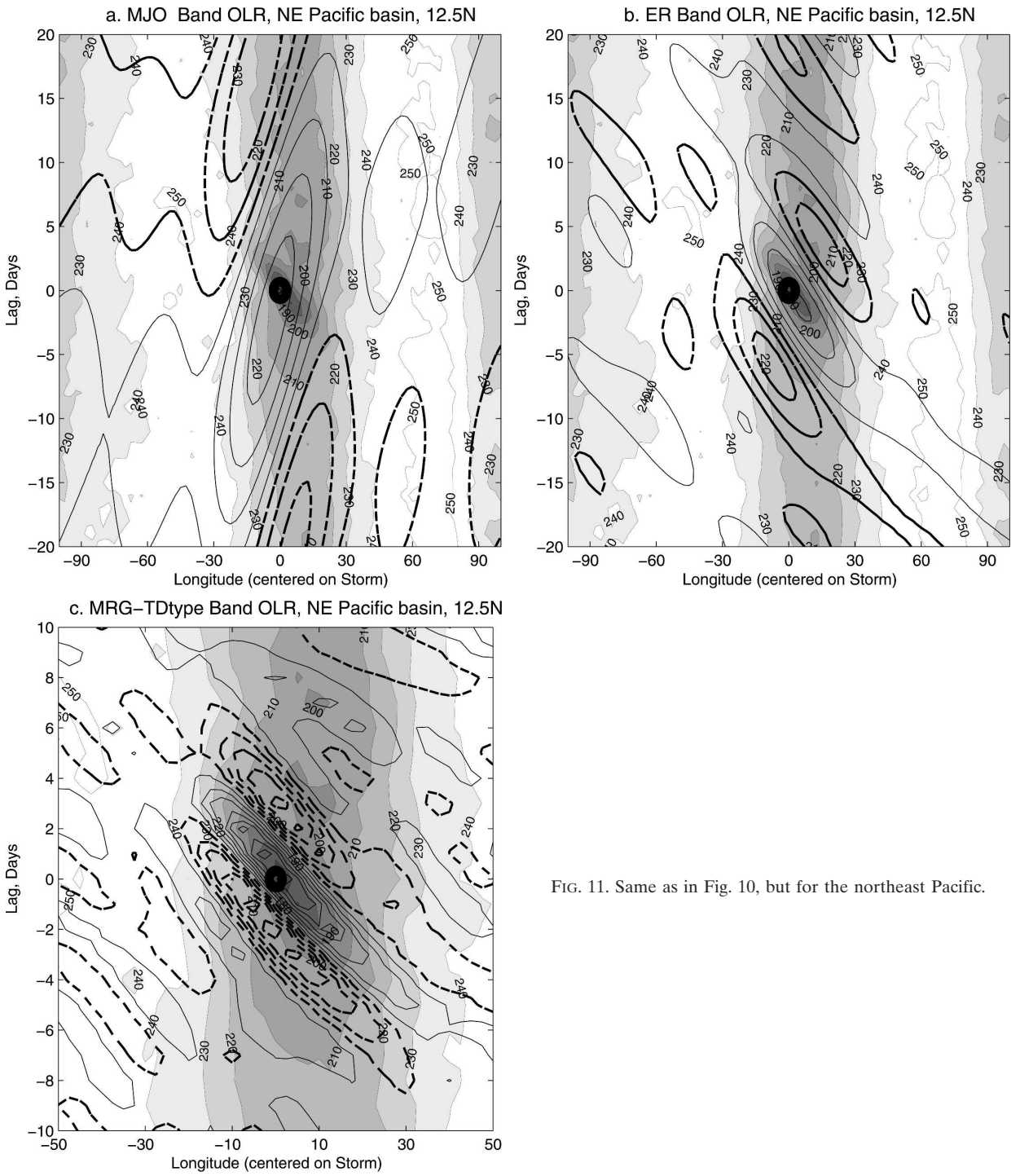

FIG. 11. Same as in Fig. 10, but for the northeast Pacific.

sphere basins, in the northwest Pacific warm-season activity does not tend to be above average in any wave band when genesis occurs. This does not mean that the waves are unrelated to genesis in the northwest Pacific, as there is a clear tendency for storms to occur in certain portions of the waves when they are present, regardless of whether they are more active than average. The two Southern Hemisphere basins behave much like the northwest Pacific in this respect. Both the south Indian and South Pacific basins show no tendency to form cyclones when the basin has enhanced MJO or ER activity. However, they do show a weak tendency

for cyclogenesis when MRG–TD-type activity is above normal. These higher-frequency waves are not as frequent or as strong in the Southern Hemisphere as they are in the Northern Hemisphere.

The basins are large, and incipient cyclones are not. Therefore, a more compelling case for wave–genesis relationships comes from analysis of wave conditions at both the time and place of genesis events. The scarcity of data over the tropical oceans makes it difficult to reliably analyze individual waves in many cases, but compositing techniques are capable of identifying mean conditions at the time of genesis.

The composites of the filtered OLR and wind anomalies relative to the genesis points yield several important, general results:

- In each of the six basins the storms form in conjunction with a wave structure that strongly resembles the expected wave structure associated with that filter band.
- In each basin the storms tend to form at nearly the same location within the composite wave structure.
- All of the composites except those for the Kelvin wave show approximate flow reversal between the 850- and 200-hPa levels, suggesting that the relevant wave structure is the baroclinic, first internal vertical mode, allowing the waves to both modulate vertical shear and to produce opposing vorticity anomalies between the lower and upper troposphere.
- All of the wave types seen in the composites are strongly asymmetric across the equator, though most of the ER composites do show opposite hemisphere circulations, consistent with theoretical wave structures.

The MJO consistently produces storms near the eastern edge and to the poleward side of the low-level westerly wind anomaly and within the eastern and equatorward portion of a cyclonic gyre. Thus, the MJO enhances both the convergence and the low-level rotation at the genesis location. (In the Southern Hemisphere the primary effect seems to be the enhancement of the rotation.) The composites also show a tendency for the MJO to cause easterly vertical shear anomalies at the genesis location in most basins, and this would tend to be favorable for storm formation. The storms also form well within the region of locally enhanced convection.

The ER waves also appear to enhance genesis by increasing both the large-scale rotation and convection, as in this band the storms form within the low-level cyclonic gyre and about two days after the wave's convective anomaly first reaches the genesis point. The ER waves also cause significant easterly shear anomalies at the genesis locations in about half of the basins. Similarly, the smaller and higher-frequency MRG–TD-type wave band shows a consistent pattern of storms forming within the region of enhanced low-level rotation and within the negative OLR (convectively enhanced) region of the wave.

Most of the world's tropical cyclones form within or very close to the circulations of MT ITCZs. This is particularly true for the two basins examined most closely in this paper (e.g., the northwest and northeast Pacific). Within these regions we hypothesize that the waves accelerate the cyclogenesis process within a climatologically favorable region. From the results of the current study it would appear that the MJO, ER, and MRG–TD-type waves all do this by enhancing the amount of large-scale convection in the region as well as the low-level rotation. The MJO and ER waves also produce a favorable easterly shear anomaly at the genesis location. These waves often modulate the time and place of cyclone formation within a monsoon trough. An unperturbed trough can eventually become unstable and break down, forming one or more cyclones (e.g., Ferreira and Schubert 1997; Wang and Frank 1999). The latter study found that simulations of an idealized monsoon trough designed to resemble conditions in the northwest Pacific during August tended to produce ITCZ breakdown after about 10–14 days. However, because monsoon troughs are almost constantly perturbed by equatorial waves, we suggest that most cyclogenesis events occur when one or more of these waves accelerate the process.

At locations that are far removed from an MT, wave-induced genesis can still occur, but the process is likely to take longer. Tropical cyclone formation from TD-type waves in the easterly trade flow is particularly common in the North Atlantic.

Last, the composite analyses show that on average, the wave anomalies associated with tropical cyclogenesis are detectable prior to genesis for all wave types and basins. The lead time is up to a month for the MJO and up to 3 weeks for the ER wave in the northeast Pacific. This holds promise for the possible use of wave indices as predictors in statistical models for forecasting the probability of tropical cyclogenesis. Preliminary tests of such procedures are ongoing and are producing encouraging results. Other wave forecasts are already being used at the Bureau of Meteorology Research Centre in Australia using procedures described in Wheeler and Weickmann (2001).

While the above analyses provide evidence that tropical cyclogenesis is frequently associated with equatorial wave perturbations, and is probably enhanced by them, much remains to be learned about the mechanisms involved. We are in the process of performing

more detailed analyses that will examine how the anomalous wave circulations affect the vorticity, vertical shear, and other conditions at the time and place of genesis. The results of this ongoing work will be presented in a future paper.

Acknowledgments. This research was supported by the National Science Foundation Grants ATM-0003351 and ATM-0233881. Professor John Molinari and two anomymous reviewers provided useful comments that dramatically improved the presentation of our results. George Kiladis graciously provided an additional review and comments.

APPENDIX

Determining the Threshold for Active Wave Periods

Though much of the activity in the wave-filtered OLR is contributed by large-scale waves, it is important to acknowledge that the storms themselves contribute to the filtered data as well. A correction for this contribution must be applied to our statistics that depend on wave activity. The contribution of the storms to variance in our filtered datasets tends to be small but can make the waves appear to be active on the genesis date when perhaps they are not. Wheeler et al. (2000) applied a wave activity threshold equal to the mean variance of their filtered wave index time series before making their regression composites, and included activity in their composites only during periods when a time series of windowed variance exceeded that threshold. We selected the same activity threshold, plus a correction estimated to be the contribution of the mean storm to variance in the band. We estimated this contribution as follows. We constructed a storm-centered mean longitude–time array of unfiltered OLR anomalies associated with all Northern Hemisphere storms in our dataset that lasted longer than 10 days. We found the mean storm-centered OLR patterns for each day of the life of the storms, giving the relevant mean temporal a well as spatial structures.

We plotted the resulting mean and did not discern any distinct wave structures other than the signature of the mean storm itself. We then applied the filters to this mean storm, squared the resulting anomalies, and passed the same moving averages over the result that we applied to calculate wave activity as discussed in the text. The estimated contribution of the storms to the variance in each wave band is just this variance estimate at the time and place of genesis. The values are 10.3, 30.2, 83, and 1.7 $(\mathrm{W\ m^{-2}})^2$ for the MJO, ER, MRG–TD-type, and Kelvin bands, respectively. Though individual storms might contribute more or less than these values because of differences between the sizes and translation speeds, our estimates are appropriate for our statistical applications. We tried an alternative method of generating an artificial storm OLR signature that would not have included any wave signal, and results were consistent with those given above.

REFERENCES

Bessafi, M., and M. Wheeler, 2006: Modulation of south Indian Ocean tropical cyclones by the Madden–Julian Oscillation and convectively coupled equatorial waves. *Mon. Wea. Rev.,* **134,** 638–656.

Bister, M., and K. A. Emanuel, 1997: The genesis of Hurricane Guillermo: TEXMEX analysis and a modeling study. *Mon. Wea. Rev.,* **125,** 2662–2682.

Briegel, L. M., 2002: The structure and variability of the ITCZ of the western North Pacific. Ph.D. dissertation, Department of Meteorology, The Pennsylvania State University, 212 pp.

——, and W. M. Frank, 1997: Large-scale influences on tropical cyclogenesis in the western North Pacific. *Mon. Wea. Rev.,* **125,** 1397–1413.

Carlson, T. N., 1969: Synoptic histories of three African disturbances that developed into Atlantic hurricanes. *Mon. Wea. Rev.,* **97,** 256–276.

Dickinson, M., and J. Molinari, 2002: Mixed Rossby-gravity waves and western Pacific tropical cyclogenesis. Part I: Synoptic evolution. *J. Atmos. Sci.,* **59,** 2183–2196.

Ferreira, R. N., and W. H. Schubert, 1997: Barotropic aspects of ITCZ breakdown. *J. Atmos. Sci.,* **54,** 261–285.

Frank, N. L., and G. B. Clark, 1980: Atlantic tropical systems of 1979. *Mon. Wea. Rev.,* **108,** 966–972.

Gray, W. M., 1968: Global view of the origin of tropical disturbances and storms. *Mon. Wea. Rev.,* **96,** 669–700.

——, 1979: Hurricanes: Their formation, structure and likely role in the tropical circulation. *Meteorology over the Tropical Oceans,* D. B. Shaw, Ed., Royal Meteorological Society, 155–218.

——, 1985: Tropical cyclone climatology. WMO Tech. Doc. WMO/TD-72, Vol. 1, WMO, Geneva, Switzerland, 145 pp.

Hall, J. D., A. J. Matthews, and D. J. Karoly, 2001: The modulation of tropical cyclone activity in the Australian region by the Madden–Julian Oscillation. *Mon. Wea. Rev.,* **129,** 2970–2982.

Hendon, H. H., and B. Liebmann, 1991: The structure and annual variation of antisymmetric fluctuations of tropical convection and their association with Rossby-gravity waves. *J. Atmos. Sci.,* **48,** 2127–2140.

Kiladis, G. N., K. H. Straub, and P. T. Haertel, 2005: Zonal and vertical structure of the Madden–Julian oscillation. *J. Atmos. Sci.,* **62,** 2790–2809.

Kurihara, Y., and R. E. Tuleya, 1981: A numerical simulation study on the genesis of a tropical storm. *Mon. Wea. Rev.,* **109,** 1629–1653.

——, and ——, 1982: Influence of environmental conditions on the genesis of a tropical storm. *Intense Atmospheric Vortices,* L. Bengtsson and J. Lighthill, Eds., Springer-Verlag, 71–79.

Landsea, C. W., 1993: A climatology of intense (or major) Atlantic hurricanes. *Mon. Wea. Rev.,* **121,** 1703–1713.

Liebmann, B., H. H. Hendon, and J. D. Glick, 1994: The relationship between tropical cyclones of the western Pacific and Indian Oceans and the Madden–Julian Oscillation. *J. Meteor. Soc. Japan,* **72,** 401–411.

Madden, R. A., and P. R. Julian, 1994: Observations of the 40–50-day tropical oscillation—A review. *Mon. Wea. Rev.,* **122,** 814–837.

Maloney, E. D., and D. L. Hartmann, 2001: The Madden–Julian Oscillation, barotropic dynamics, and North Pacific tropical cyclone formation. *J. Atmos. Sci.,* **58,** 2545–2558.

Matsuno, T., 1966: Quasi-geostrophic motions in the equatorial area. *J. Meteor. Soc. Japan,* **44,** 25–43.

McBride, J. L., and R. M. Zehr, 1981: Observational analysis of tropical cyclone formation. Part II: Comparison of non-developing vs. developing systems. *J. Atmos. Sci.,* **38,** 1132–1151.

Molinari, J., and D. Vollaro, 2000: Planetary and synoptic-scale influence on eastern Pacific tropical cyclogenesis. *Mon. Wea. Rev.,* **128,** 3296–3307.

Reed, R. J., D. C. Norquist, and E. E. Recker, 1977: The structure and properties of African waves disturbances as observed during phase III of GATE. *Mon. Wea. Rev.,* **105,** 317–333.

Ritchie, E. A., and G. J. Holland, 1999: Large-scale patterns associated with tropical cyclogenesis in the western Pacific. *Mon. Wea. Rev.,* **127,** 2027–2043.

Roundy, P. E., and W. M. Frank, 2004a: A climatology of waves in the equatorial region. *J. Atmos. Sci.,* **61,** 2105–2132.

——, and ——, 2004b: Effects of low-frequency wave interactions on intraseasonal oscillations. *J. Atmos. Sci.,* **61,** 3025–3040.

Straub, K. H., and G. N. Kiladis, 2002: Observations of a convectively coupled Kelvin wave in the eastern Pacific ITCZ. *J. Atmos. Sci.,* **59,** 30–53.

Takayabu, Y. N., 1994: Large-scale cloud disturbances associated with equatorial waves. Part I: Spectral features of the cloud disturbances. *J. Meteor. Soc. Japan,* **72,** 433–448.

Thorncroft, C., and K. Hodges, 2001: African easterly wave variability and its relationship to Atlantic tropical cyclone activity. *J. Climate,* **14,** 1166–1179.

Wang, H., and W. M. Frank, 1999: Two modes of tropical cyclogenesis: An idealized simulation. Preprints, *23d Conf. on Hurricanes and Tropical Meteorology*, Dallas, TX, Amer. Meteor. Soc., 923–924.

Wheeler, M., and G. N. Kiladis, 1999: Convectively coupled equatorial waves: Analysis of clouds and temperature in the wavenumber-frequency domain. *J. Atmos. Sci.,* **56,** 374–399.

——, and K. Weickmann, 2001: Real time momitoring of modes of coherent synoptic to intraseasonal convective variability. *Mon. Wea. Rev.,* **129,** 2677–2694.

——, G. N. Kiladis, and P. J. Webster, 2000: Large-scale dynamical fields associated with convectively coupled equatorial waves. *J. Atmos. Sci.,* **57,** 613–640.

Zehr, R. M., 1992: Tropical cyclogenesis in the western North Pacific. NOAA Tech. Rep. NESDIS 61, 181 pp. [Available from the U. S. Department of Commerce, NOAA/NESDIS, 5200 Auth. Rd., Washington, DC 20233.]

Zhang, C., and P. J. Webster, 1989: Effects of zonal flows on equatorially trapped waves. *J. Atmos. Sci.,* **46,** 3632–3652.